Advances and Prospects of Fiber Supercapacitors

S. T. Senthilkumar, Yu Wang, and Haitao Huang*

Department of Applied Physics, The Hong Kong Polytechnic University, Hong Kong SAR, China.

aphhuang@polyu.edu.hk (H.Huang)

Abstract

Flexible fiber electronic devices have attracted extensive research interest in the past few years due to their unique features and potential applications in the next generation wearable electronics and/or smart textiles. Various fiber-type energy storage devices are highly demanded to store or power the available fiber electronic devices. Among them, supercapacitors (SCs) act as a promising candidate that can offer long cycle life, high power density, safety and so on. This review article explores the recent research progress in the development of both symmetric and asymmetric fiber SCs, their configurations and fabrication designs. A broad overview is given to the design of various fiber electrode materials along with their performance and characterizations for the fabrication of flexible fiber SCs. Finally the current challenges and future perspectives for the development of high performance flexible fiber SCs are highlighted.

Keywords: Fiber Supercapacitor; Wearable; Flexible; Energy Density; Power Density

1. Introduction

Flexible electronics devices such as displays, sensors, transistor, solar cells (photovoltaic cells), and thermoelectric generators have attracted more and more attention in the modern world for various applications [1–5]. However, the conventional type electronic devices are very rigid, heavy and bulky and hence they do not meet the requirement for flexibility, foldability and conformability [6]. Last decade has witnessed the fast and extensive development of planar-type flexible electronic devices which are light weight, flexible and portable. However, they need further improvements for wearable (e-textiles or smart textiles) and stretchable device applications.

Nowadays, there are many reports on flexible fiber electronic devices (i.e., transistors, sensors, fuel cells, solar cells, thermoelectric power generators and piezoelectric generators (nanogenerators)) [7–9]. It is hoped that these fiber electronic devices can satisfy the above application needs since they can be easily woven into any desired shape or be knitted into fabrics. To power a wire/cable type senor or transistor and to store produced energy from fuel cells, solar cells, thermoelectric power generator or piezoelectronic devices (nanogenerators), similar kinds of fiber-type flexible powering or energy storage devices are necessary [6]. Therefore, the development of fiber-type powering or energy storage devices is highly demanding and may open up a new avenue in the area of energy storage devices.

Since supercapacitors (SCs) have the salient future for various applications, such as mobile phones, wearable electronics, and flexible displays, thanks to their good life time, light weight, low cost and safety [10,11], they have been extensively investigated in the last few years [10–13]. Commonly, they are fabricated in basic planar or two-dimensional (2D) configuration and widely used for flexible electronic device applications. Generally, the flexibility of the planar SCs highly depends on electrode substrate. Different kinds of planar-type electrode substrates have been used to develop flexible SCs, such as, metal coated

plastics, conductive papers, carbon material coated cloth and conductive carbon fiber cloths or fabrics [13]. Unfortunately, those electrode substrates do not provide sufficient flexibility to satisfy the demands for future flexible wearable electronic devices and thus cannot be easily woven into textiles. They usually occupy more space and are uncomfortable for human, with air flow or convection being blocked when the planar-type devices are fixed on textile or cloth, and they also do not meet the light weight requirement for application [14]. To tackle these problems, remarkable efforts in the design of SCs have been shifted from planar (2D) to fiber (1D) format with light weight and more flexibility. Various kinds of fiber-type electrodes (CNT yarn and graphene yarn, etc.,) have been developed or used on fiber substrates (carbon fiber, metal wire etc.,) for the fabrication of fiber SCs [15–18] because these fiber electrodes provide the maximum flexibility to be integrated into textile or wearable devices.

Although there are many reviews on the conventional planar-type flexible SCs, there is no broad review on the recently emerged fiber-type flexible SCs. In this regard, the present review will focus on the most recent progress in fiber SCs which will be the hot spot of research in the future. It also highlights the future perspectives for the development of flexible fiber SCs.

2. The birth and development of fiber SCs

The prototype fiber supercapacitor (SC) was first fabricated by Bae *et al*. [19] using ZnO nanowire (NW) coated fiber electrode in 2011 and their device architecture is shown in Figure 1a. Unfortunately, their architecture has the drawback of short circuit via direct contact of the two fiber electrodes during bending owing to the double twisted structure, together with the low capacitance, low energy density and poor power density. In 2012, a tri-helix architecture which consists of two working electrodes and a spacer wire has been developed (Figure 1b) by Fu *et al*. [16] to avoid the short circuit problem.

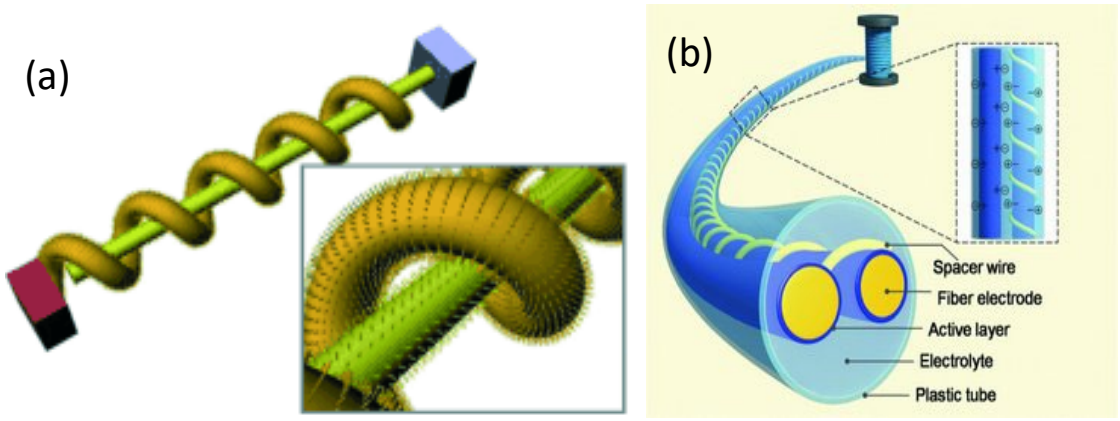

Figure 1 Schematic diagram of (a) prototype fiber SC and (b) the tri-helix architecture fiber SC. Reproduced with permission [16,19].

Here the spacer wire plays a vital role in avoiding the short circuit of the device (Figure 1b), but the capacitance is low due to the parallel-type structure and the low conductivity of plastics wire (current collector). Efforts to improve the conductivity by using metal wire/fiber current collectors have restricted the flexibility and increased the weight of the device. Later in 2012, in order to achieve a high flexibility and light weight device, carbon fibers (for examples, CNT yarn and graphene fibers) [15,16] are widely employed as fiber electrodes and they also act as current collectors because of their conductive nature. Besides, the light weight of carbon fiber is also beneficial to the device's gravimetric capacitance. Moreover, gel electrolyte has become another important component of much research for flexible SCs since it is very convenient to handle, non-flammable, low toxicity, and reliable for a wide range of operation temperatures [20]. In addition to that, the polymer electrolyte can circumvent the leakage problem and reduce the device packaging cost and, at the same time, it can also act as a separator to avoid short circuit in device [20,21]. There are two kinds of commonly studied polymer based electrolytes for SCs, solid-state polymer electrolyte and gel polymer electrolyte. Gel polymer electrolytes normally have better ionic conductivity (10^{-3} to 10^{-4} S cm^{-1}) than solid ones (10^{-7} to 10^{-8} S cm^{-1}) due to the existence of a large amount of water in the polymer matrix that improves the ionic conductivity [20–22]. The most

commonly used polymer host materials for gel electrolytes are polyacrylate (PAA), poly(ethylene oxide) (PEO), poly(vinyl alcohol) (PVA), polyacrylonitrile (PAN), poly(vinylidene fluoride) (PVdF), poly(vinylidene fluoride-co-hexafluoropropylene) (PVdF-co-HFP), poly(methyl methacrylate) (PMMA), poly-(ethylene glycol) blended poly(acrylonitrile) (PAN-b-PEG-b-PAN) and poly(amine-ester) (PAE) [20–22]. In the case of fiber SCs, PVA based hydrogel electrolytes are extensively studied, such as, PVA/H_2SO_4/H_2O, PVA/H_3PO_4/H_2O, PVA/KOH/H_2O, PVA/KCl/H_2O and so on, as PVA is the widely inspected polymer that has low cost, good electrochemical stability, good mechanical properties and non-toxic nature [21,22]. The major architectures reported in the last few years, especially in 2012, are given below (Figure 2) with a brief description.

(a). Parallel-like type:

Parallel-like fiber SC is fabricated by keeping the two electrodes closely in parallel with a separator (spacer) or gel polymer electrolyte (Figure 2a) [18].

(b). Coaxial type:

It is assembled by a core fiber electrode and an outer layer electrode (which is developed via layer-by-layer coating) with a separator or gel polymer electrolyte between them (Figure 2b) [23].

(c). Two-ply type:

It is constructed by twining and twisting two fiber electrodes together with a separator or gel polymer electrolyte between them (Figure 2c) [24].

(d). Coaxial-helix type:

It is made up by inserting a fiber electrode into a coil-like fiber electrode or winding a fiber electrode into a coil on a stable fiber electrode with a separator or gel polymer electrolyte (Figure 2d) [25].

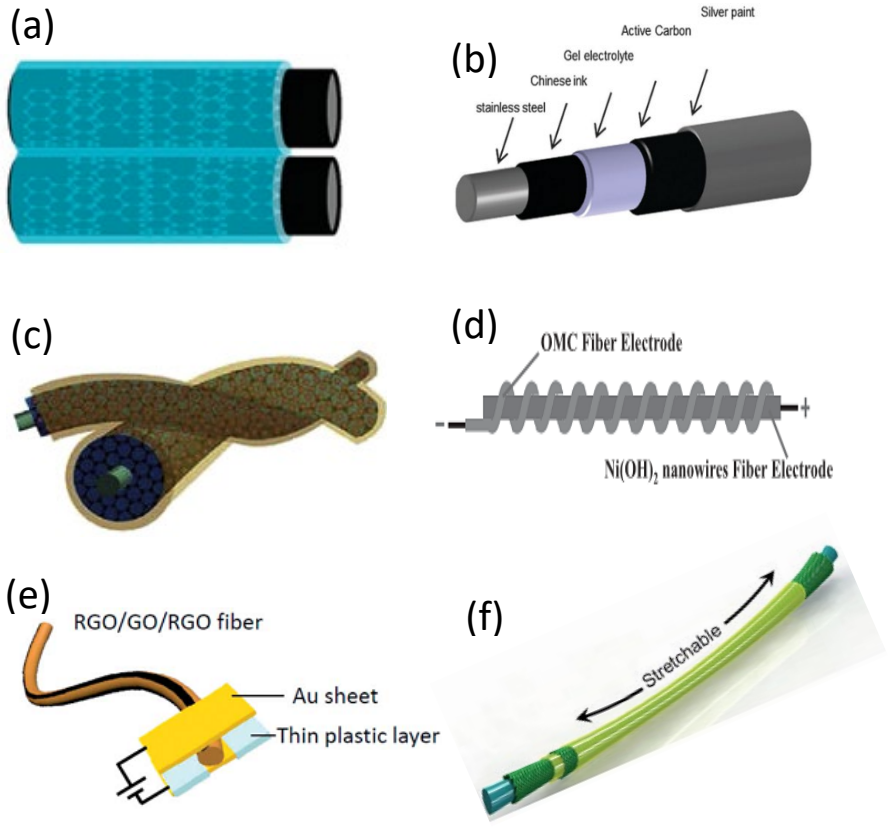

Figure 2 Schematic diagrams of different fiber SC architectures: (a) parallel-like type [18], (b) coaxial type [23], (c) two-ply type [24], (d) coaxial-helix type [25], (e) all-in one type [26] and (f) Coaxial stretchable type [27]. Reproduced with permission [18, 23-27].

(e). All-in-one fiber-type:

In an all-in-one fiber SC, the two electrodes and the separator are rationally integrated into a single fiber without any extra bonding agent or assembly process involved (Figure 2e) [26].

(f). Coaxial stretchable type:

It is assembled by wrapping electrode materials onto the elastic fiber with gel electrolyte where the elastic fiber enables the stretchability (Figure 2f) [27].

3. Symmetric fiber SCs

Commonly, symmetric SCs are fabricated by using the same electrode material in both positive and negative electrodes. The symmetric fiber SCs can be classified into three main categories based on the electrode materials, i.e., carbon based fiber SCs, pseudocapacitive (redox) fiber SCs and composite (carbon and pseudocapacitive material) based fiber SCs.

3.1. Carbon (capacitive) based fiber SCs

Generally, carbon based SCs can store the charges or ions electro-statically (non-faradic process) by forming an electric double layer (EDL) [28b] at the electrode/electrolyte interface so that this kind of carbon SCs are called electric double layer capacitors (EDLCs) [28b,29] Activated carbon, carbon nanotubes (single-walled carbon nanotubes (SWCNT) and multi-walled carbon nanotubes (MWCNT)), and graphene, etc., are the most commonly used carbon based materials in conventional SCs [28b–30] since these carbon based electrode materials are lightweight, low-cost, easy to handle, electrically conductive, thermally and chemically stable (in acidic and alkali solutions), and they have wide operating temperature range and large surface area [31-32b]. In fiber SCs, carbon based fibers such as single-walled or multi-walled carbon nanotube fibers [33,34], graphene fibers [17], carbon fibers [35], and carbon-carbon composite fibers [36] are the most attractive owing to their one-dimensional (1D), flexible and conductive features [37]. The general charge storage process of the carbon materials in the fiber SCs can be described as,

$$C + nX \leftrightarrow C||nX \quad (1)$$

where, X is a cation or anion and || indicates the electric double layer (EDL). The main types of carbon fiber SCs are summarized below and their key performances are listed in table 1.

3.1.1. Carbon Nanotube (CNT) based fiber SCs

Carbon Nanotubes (CNTs) are used as promising electrode material for SCs due to their unique one dimensional structure with good electrical conductivity that facilities the rapid charge transport as well as high mechanical strength [36] and light weight. In the early stage, CNT based fiber electrodes were prepared by coating CNTs on the surface of fiber substrate (such as metal wire [38]) to fabricate fiber SC. Later, CNT fibers were used both as electrode

and current collector in fiber SCs [33,34]. Normally, CNT fibers are produced by four methods, (a) spinning from CNT solution, (b) spinning from a vertically aligned CNT array grown on a substrate, (c) spinning from a CNT aerogel formed by chemical vapor deposition (CVD) and (d) twisting/rolling from a CNT film [39]. These flexible CNT fibers have several advantages, [40] such as, low density of 1 g cm^{-3} (or 10 µg m^{-1}), high tensile strength up to 10^3 MPa and high electrical conductivity up to 10^3 S cm^{-1}.

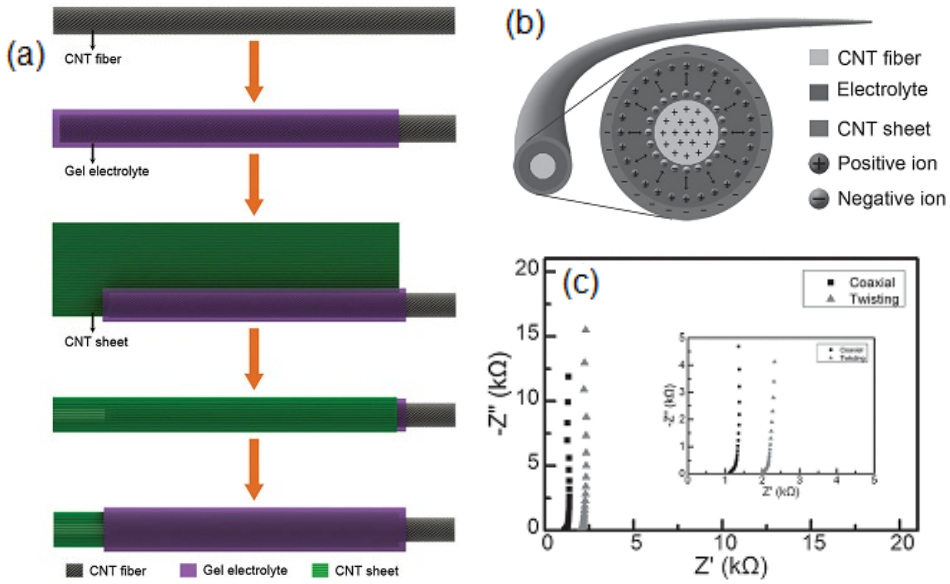

Figure 3 (a) Schematic diagram showing the fabrication of a coaxial fiber SC with CNT fiber and CNT sheet as the two electrodes, (b) Schematic diagram showing the cross-sectional structure and the mechanism of charge storage in the coaxial fiber SC. The electropositive CNT fiber and electronegative CNT sheet functioned as the positive and negative electrodes, respectively and (c) Nyquist plots of the SCs with both coaxial (square dots) and twisted (triangular dots) structures. Reproduced with permission [33].

In 2013, a coaxial fiber SC was fabricated by Chen *et al*. [33] from an aligned CNT fiber and CNT sheet with the help of a polymer gel (Figures 3a and b). Here, the CNT fiber and sheet were dry-spun from CNT arrays that had been synthesized by CVD and they showed an electrical conductivity on the level of (10^2 –10^3) S cm^{-1} and a tensile strength on the order of (10^2 –10^3) MPa. One of the advantages of this unique coaxial structure is that it can reduce the contact resistance between the two electrodes and a lower internal resistance

has been observed in the Nyquist plots (Figure 3c). Meantime, this structure also provides more effective area for ion storage. This fiber SC has achieved a much higher discharge capacitance of 59 F g^{-1} (32.09 F cm^{-3}, 29 μ F cm^{-1} or 8.66 mF cm^{-2}) than that of the SC designed by twisting two CNT fibers together (4.5 F g^{-1}). These SC fibers exhibit energy densities up to 1.88 Wh kg^{-1} and power densities up to 755.9 W kg^{-1}.

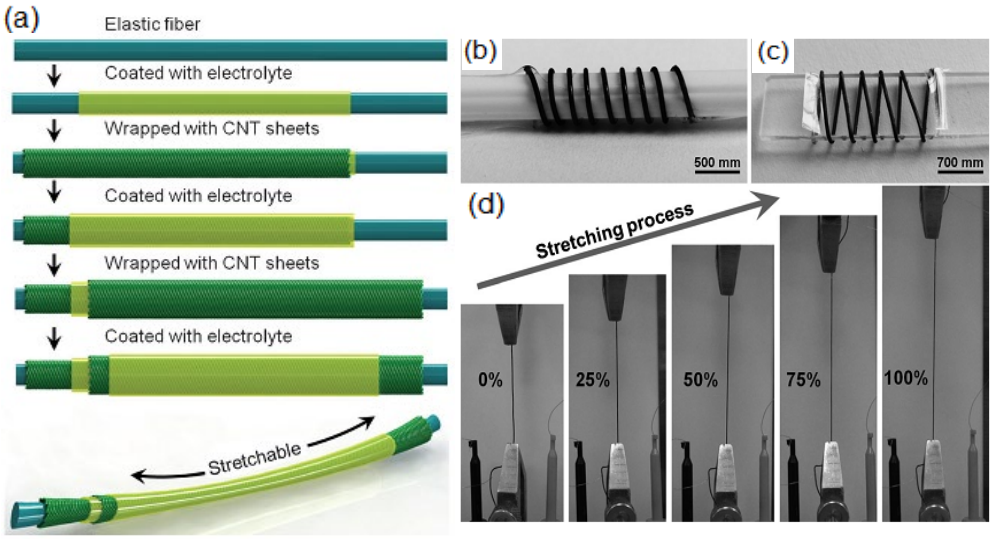

Figure 4 (a) Illustration of the fabrication of a highly stretchable, fiber SC with a coaxial structure, (b and c) Photographs of two fiber SCs wound on different shapes of substrates and d) Photograph of the fiber SC under different strains of 0%, 25%, 50%, 75%, and 100%. Reproduced with permission [27].

Developing stretchable flexible fiber SC has drawn great attention and rapid advancement has been made. For example, Xu *et al.* [41] first fabricated (in 2014) the stretchable fiber SCs using CNT fibers (with a diameter of 15 μm) which were spun from a vertically aligned CNT array, and gel electrolyte (PVA/H_2SO_4). To make the fibers highly stretchable, they glued the CNT fibers on spandex or elastane synthetic fiber which can be elongated up to 500 to 800%. The maximum volumetric capacitance delivered by the stretchable fiber SC is 13.5 F cm^{-3}. However, further modification is required to obtain a stable fiber SC with good stretchability. Later, Yang and co-worker [27] developed a reliable and stretchable fiber SC by wrapping CNT sheets around elastic fibers (Figure 4a). The CNT

sheets were synthesized by CVD and they offer high flexibility, tensile strength, electrical conductivity, and mechanical and thermal stabilities. It is found that by increasing the thickness of the CNT sheet from 110 to 330 nm, the specific capacitance was increased from 11.0 to 19.2 F g^{-1}, due to the decreased electrical resistance of the CNT sheet electrode. Further increasing the thickness to 550 nm reduced the capacitances to 11.3 F g^{-1} because the gel electrolyte cannot be efficiently infiltrated into thick CNT sheet electrode. The fiber SC maintains a high specific capacitance of ~18 F g^{-1} after being stretched by 75 % for 100 cycles. In addition, the fabrication process can be easily scaled up while keeping the flexible and stretchable SCs with high efficiency and low cost (Figures 4 b-d).

3.1.2. Graphene based fiber SCs

Graphene is another choice of light weight electrode material for SC applications, which has favourable properties such as good electrical conductivity even at room temperature, good mechanical flexibility, high surface area (2675 m^2 g^{-1}) and low preparation cost [42a-42d]. It can offer a maximum theoretical specific capacitance of 550 F g^{-1} [42,43]. It can be prepared via different methods, such as, laser irradiation, mechanical exfoliation, liquid-phase exfoliation, hydrothermal reaction, chemical or electrochemical reduction, CVD and so on, where graphene oxide (GO) is the major source to obtain graphene [44–47]. Though it has been extensively studied for applications in planer-type SCs, it is still in its infancy in fiber SCs.

Graphene based fiber SC designed by Li *et al.* [48a] was prepared by coating graphene on Au wire through electrochemical method to form a graphene fiber electrode. In this technique, under the application of an electric field, GO sheets are deposited on the surface of the Au wire and get reduced. This electrochemical technique is considered to be low cost, fast and convenient for industrialization to obtain a graphene fiber electrode. The calculated capacitance of the fiber SC per unit length or per unit area was 11.4 μF cm^{-1} or

0.726 mF cm^{-2}. However, the Au wire used is expensive and exhibits low flexibility. Cao *et al*. [18] replaced the Au wire by carbon fiber, taking advantages of good strength, high flexibility, low cost and good conductivity of the carbon fiber. The fabricated SC achieved a high length specific capacitance of 13.5 mF cm^{-1} at a current density of 0.05 mA cm^{-1} and it was claimed that the fabricated fiber SC was applicable for large scale production for practical usage. Liu *et al*. [48b] coated Ni metal on the cotton yarn and make it as a conductive yarn substrate instead of using a metal wire. Then, graphene was immobilized on the Ni coated cotton yarn and used as a fiber electrode in a fiber SC. The device exhibited good electrochemical performance with energy and power densities of 6.1 mWh cm^{-3} and 1400 mW cm^{-3}, respectively. The electrochemical performance was tested via serial and parallel connections as well.

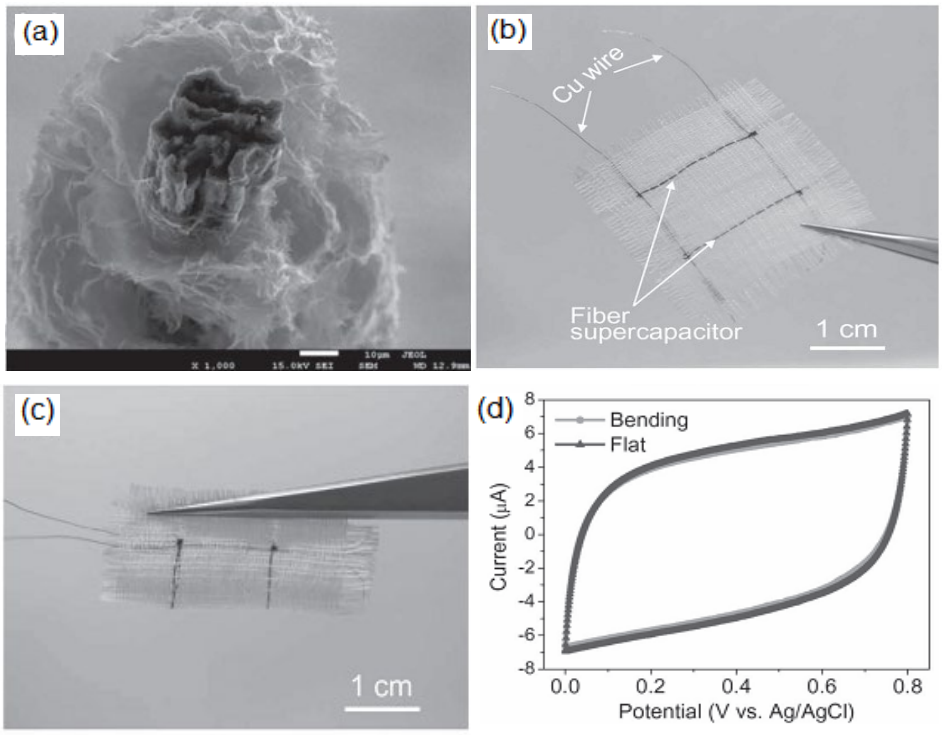

Figure 5 (a) Cross-section view of a GF@3D-G showing the core GF surrounded by vertically standing graphene sheets, (b and c) Photos of the textile embedded with two GF@3D-G fiber SCs in flat and bending state, respectively and (d) CV curves of two GF@3D-G fiber SCs as the textile in flat (a) and bending (b) states with a scan rate of 50 mV/s. Reproduced with permission [50].

Graphene fibers (GFs) are of great interest recently because they not only possess the mechanical flexibility as common fibers do, but also are low cost, light weight, and easy to be functionalized. GFs are obtained through (a) wet spinning of graphene oxide (GO) liquid crystal phases, (b) dimensional-confined hydrothermal strategy, (c) chemical vapor deposition (CVD)-assisted process (d) spontaneous reduction and assembly of GO and (e) electrophoretic self-assembly [49]. These GFs fibers exhibit high electrical conductivity of about 10-285 S cm^{-1} [50]. Meng *et al*. [50] used GF as the fiber electrode which was prepared via a facile one-step dimensionally-confined hydrothermal strategy from aqueous suspensions. Astonishingly, the prepared GF has a density of 0.23 g cm^{-3} which was 1/7 and 1/85 that of conventional carbon fiber (> 1.7 g cm^{-3}) and Au wire (ca. 20 g cm^{-3}), respectively. It was reported that this GF had better electric conductivity of 10 S cm^{-1}. To improve their electrochemical performances, 3D graphene (3D-G) network (GF@3D-G) was developed on the GF fibers (Figure 5a) using electrochemical method and this 3D framework can partially overcome the problem of restacking and aggregation of graphene sheets [51]. The constructed GF@3D-G fiber SC delivered a high mass-specific capacitance of ~25–40 F g^{-1} and area-specific capacitance of ~1.2–1.7 mF cm^{-2}. They can be woven into textile (Figures 5b-d) with stable electrochemical performance at bending and flat states (Figure 5d). Very recently, coaxial graphene fiber SC was designed [52], where the core electrode was prepared by a wet-spinning technique and the outer core electrode was prepared by a dip coating method. A specific capacitance of 205 mF cm^{-2} (182 F g^{-1}) and an energy density of 17.5 μW h cm^{-2} (15.5 W h kg^{-1}) were achieved.

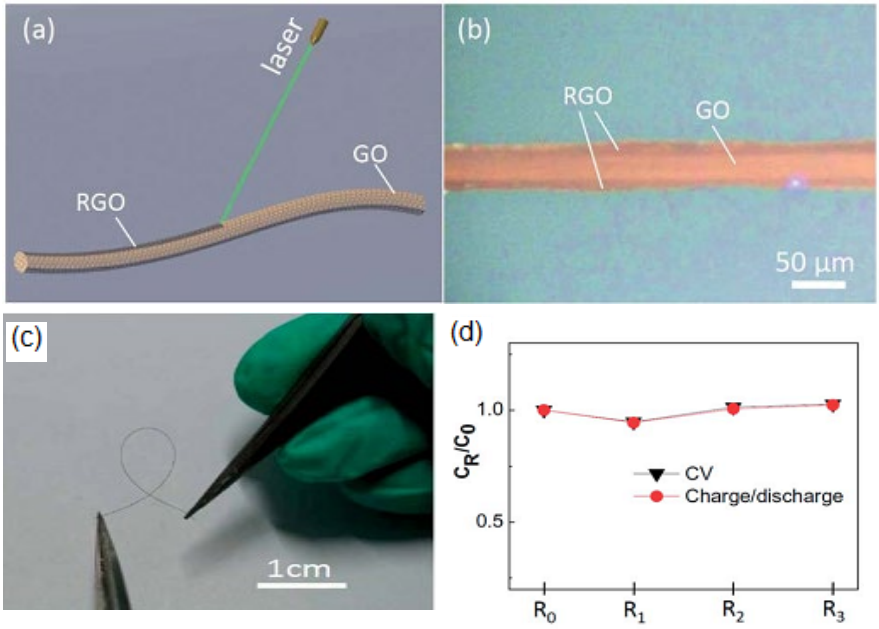

Figure 6 (a) Schematic of the laser reduction of GO fiber for the formation of RGO-GO-RGO fiber, (b) optical image of the RGO-GO-RGO fiber under a microscope, (c) photo image of the RGO-GO-RGO fiber under arbitrary tortuosity and (d) capacitance ratio of the RGO-GO-RGO fiber SC at the bending state vs. the initial state (where, R along *x*-axis represents the radius of curvature of RGO-GO-RGO fiber SC, i.e., R_o=1mm (initial state), R_1=24mm, R_2=13mm and R3=7.5mm). Reproduced with permission [26].

In 2014, a new kind of all-in-one single fiber SC has been made by a region-specific laser reduction of a GO fiber into a sandwiched reduced GO-GO-reduced GO (RGO–GO–RGO) configuration [26]. This all-in-one single fiber SC has rationally integrated the two electrodes (RGO) and the separator (GO) within one single GF (Figure 6) without the use of any bonding agent or assembly process. The RGO–GO–RGO fiber SC reaches a capacitance as high as 1.2 mF cm^{-2} under a current density of 80 mA cm^{-2}. The fiber SC maintains high capacitance under bending state (Figures 6 c and d).

Table 1: Performance of recently reported carbon based fiber SCs

Device configuration and cell voltage	Electrolyte	Capacitance	Energy density and Power density	Cycle life	Ref.
CNT based fiber SCs					
Coaxial and 1 V	PVA-H_3PO_4	59 F g^{-1} (32.09 F cm^{-3}, 29 μ F cm^{-1} or 8.66 mF cm^{-2}	1.88 Wh kg^{-1} and 755.9 W kg^{-1}	88.4 % for 11000 cycles	[33]
Twisted and 0.8 V	PVA-H_2PO_4	13.5 F cm^{-3} (4.28 mF cm^{-2})	0.226 μWh cm^{-2} (0.601 mWh cm^{-3}) and 0.493 mW cm^{-2} (1320 mW cm^{-3})	92 % for 10000 cycles	[41]
Coaxial (stretchable) and 0.8 V	PVA-H_3PO_4	20 F g^{-1}	0.515 Wh kg^{-1} and 9 W kg^{-1}	~100 % for 1000 cycles	[27]
Graphene based fiber SCs					
Parallel and 1 V	PVA-H_3PO_4	11.4 μF cm^{-1} or 0.726 mF cm^{-2}	---	---	[48a]
Parallel and 0.8 V	PVA/LiCl	---	6.1 mWh cm^{-3} and 1400 mW cm^{-3}.	~82% for 10000 cycles	[48b]
Parallel and 1 V	PVA-H_3PO_4	13.5 mF cm^{-1} (307 mF cm^{-2})	1.9 μWh cm^{-1} (13.1 μWh cm^{-2}) and 27.2 μW cm^{-1} (8.5 mW cm^{-2})	~85 % for 5000 cycles	[18]
Twisted and 1 V	PVA-H_2SO_4	40 F g^{-1} (1.7 mF cm^{-2})	1.7×10^{-7} Wh cm^{-2} and 100 μW cm^{-2}	---	[50]
Coaxial and 0.8 V	PVA-H_2SO_4	205 mF cm^{-2} (182 F g^{-1})	17.5 μW h cm^{-2} (15.5 W h kg^{-1})	100 % for 10000 cycles	[52]
All-in-one and 1 V	Not used any electrolyte	1.2 mF cm^{-2}	5.4 $\times10^{-4}$ Wh cm^{-2} and 3.6×10^{-2} W cm^{-2}	---	[26]
Carbon-carbon composite based fiber SCs					
Twisted and 1 V	PVA-H_3PO_4	1.91 mF cm^{-1} (39.7 mF cm^{-2})	0.085 μWh cm^{-1} (1.77 μWh cm^{-2}) and 0.00155 mW cm^{-1} (0.032 mW cm^{-2})	87 % for 500 cycles	[36]
Twisted and 0.8 V	PVA-H_3PO_4	~31.50 F g^{-1} (4.97 mF cm^{-2} or 27.1 μF cm^{-1})	---	---	[40]
Twisted and 0.8 V	PVA-H_3PO_4	177 mF cm^{-2} (158 F cm^{-3} and 5.3 mF cm^{-1})	3.84 μWh cm^{-2} (3.5 mWh cm^{-3}) and 0.02 mW cm^{-2} (0.018 W cm^{-3})	---	[53]
Other carbon based fiber SCs					
Coaxial and 0.8 V	PVA-H_3PO_4	3.18 mF cm^{-2} (0.1 mF cm^{-1})	---	---	[23]
Coaxial and 1 V	PVA-H_3PO_4	6.3 mF cm^{-1} (86.8 mF cm^{-2})	0.7 μWh cm^{-1} (9.8 μWh cm^{-2}) and 13.7 μW cm^{-1} (189.4 μW cm^{-2}),	94 % for 1000 cycles	[34]

3.1.3. Carbon-carbon composite based fiber SCs

Carbon-carbon composite fiber electrodes, for example, CNT/graphene [53, 54] and CNT/ordered mesopores carbon (OMC) [36], are gaining increasing interest because they combine the advantages of the two individual materials, beneficial for high performance SCs.

The CNT fiber used in the composite electrode helps increase the charge transport due to its unique one-dimensional structure with high electrical conductivity. However, the CNTs used are mostly randomly oriented with a lot of boundaries among them that hinder the charge transport. Moreover, the accessible surface area for electrolyte also needs to be improved [36,40,54,55a].

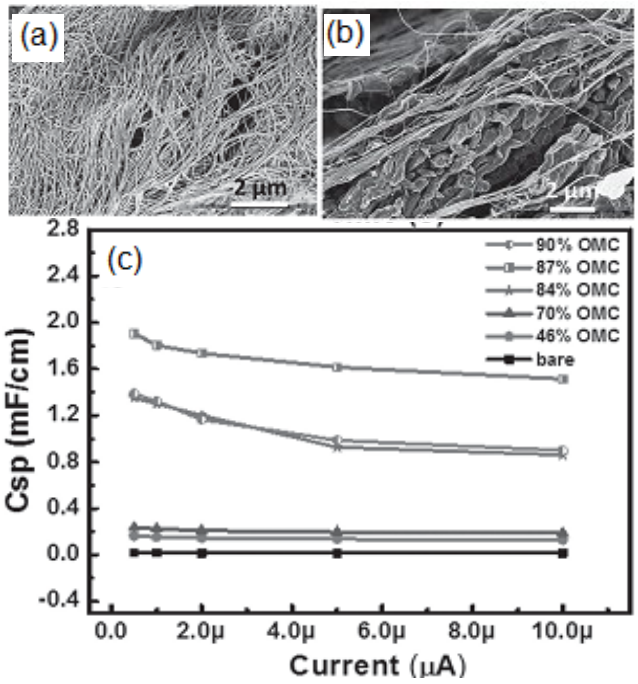

Figure 7 (a) SEM images of bare MWCNT fiber, (b) Composite fibers with 87wt.% of OMC and (c) Dependence of specific capacitance on discharging current for EDLCs composed of bare and composite MWCNT fibers with different OMC weight percentages. Reproduced with permission [36].

Flexible and bendable multi-walled CNT (MWCNT)/OMC composite fiber was (Figure 7a and b) developed [36] with the high specific surface area (1014 m^2 g^{-1}) OMC for high specific capacitance. The maximum specific capacitance of 39.67 mF cm^{-2} (or 1.907 mF cm^{-1}) was obtained for 87wt.% of OMC, nearly 20 times higher than that of the pristine MWCNT fibers (1.97 mF cm^{-2} or 0.017 mF cm^{-1}) (Figure 7c). Nevertheless, the OMC normally has a low electrical conductivity which resulted in low capacitance retention of 87% at 500 cycles.

Hybrid MWCNT/graphene yarn (Foroughi *et al.*) [54] was produced by using CNT as a host material and dispersed graphene as the guest. Topical reports reveals that hybrid materials of the 1D CNTs and 2D graphene sheets exhibit synergistic effects [55a] and result in improved electrical conductivity, thermal conductivity, mechanical flexibility and electrochemical properties when compared with pristine MWCNT or graphene. The high electrical conductivity achieved for MWCNT/graphene is over 900 S cm^{-1}, while for pristine MWCNT yarn and graphene paper, the conductivities are 220 and 72 S cm^{-1}, respectively. The ultimate tensile strength, elastic modulus and elongation at break of MWCNT/graphene were 140 ± 10 MPa, 2.58 ± 0.3 GPa and 6 ± 2%, respectively. The elongation at break of the MWCNT/graphene yarn was 100% higher than the pristine MWCNT yarn (3±2%). The elastic modulus of MWCNT/graphene yarn is relatively low compared to pristine MWCNT yarn owing to the porous nature of the MWCNT/graphene yarn. The MWCNT/graphene yarn has a specific capacitance of 111 F g^{-1}, 425% higher than the pristine MWCNT yarn [54]. Likewise, Sun *et al*. [40] have prepared the CNT/GO composite fiber with a tensile strength of ~610 MPa, higher than that of a bare CNT fiber (~500 MPa) since the GO sheets served as cross-linking components to stabilize the neighbouring CNTs. Interestingly, when RGO was used, the tensile strength increased to ~630 MP since the RGO can more effectively interact with CNTs through the strong π-π interactions to transfer the load. However, bare graphene fiber had a lower tensile strength of ~320 MPa. The CNT/RGO composite fiber showed a high conductivity of 450±20 S cm^{-1} where the graphene sheets served as conducting "bridges" to reduce the contact resistances. For comparison, the conductivities were 370±15 and 368±22 S cm^{-1} for bare CNT and CNT/GO, respectively. The maximal specific capacitance achieved was ~31.50 F g^{-1} (4.97 mF cm^{-2} or 27.1 μF cm^{-1}) for CNT/RGO composite fibers at a current density of 0.04 A g^{-1}, while it was ~5.83 F g^{-1} (0.90 mF cm^{-2} or 5.1 μF cm^{-1}) for bare CNT fibers.

Kou *et al*. [53] prepared a novel fiber electrode, the coaxial RGO/CNT/sodium carboxymethyl cellulose (CMC) yarn where the CMC was an electrically insulating porous polyelectrolyte outer layer. This polymeric sheath avoided the short circuit of fibers when they were intertwined together, while allowing ions to easily go through from the electrolyte matrix to electrodes. The SC displayed a high specific capacitance of 177 mF cm^{-2} (158 F cm^{-3} and 5.3 mF cm^{-1}) at a current density of 0.1 mA cm^{-2}. It also possessed a high energy density of 3.84 μWh cm^{-2} (3.5 mWh cm^{-3}), while the power density was 0.02 mW cm^{-2} (0.018 W cm^{-3}).

3.1.4. Other carbon based fiber SCs

In the above mentioned work, the positive and negative electrodes are of the same materials, such as CNT//CNT and graphene//graphene, except that Harrison *et al*. [23] designed a coaxial fibre SC using Chinese ink as the inner electrode and activated carbon as the outer electrode (Figure 2b). This SC was developed by simple dip-coating process and the specific areal (length) capacitance was 3.18 mF cm^{-2} (0.1 mF cm^{-1}). Remarkably, a 70 cm length of the fiber SC was fabricated and integrated into fabric. Later, Le and co-workers [34] developed a coaxial-cable type SC using two different carbon electrodes with MWCNTs coated carbon micro fiber (CMF) as the core electrode and carbon nano-fiber film as the outer electrode (Figure 8a). The recorded charge-discharge curves were almost linear, revealing their EDLC behaviour (Figure 8b). The fiber SC can reach a maximum specific capacitance and high energy density of 6.3 mF cm^{-1} (86.8 mF cm^{-2}) and 0.7 μWh cm^{-1} (9.8 μWh cm^{-2}) (Figure 8c and d), respectively, due to large effective surface area of the coaxial structure and high conductivity of MWCNT/CMF composite. Four fiber SCs connected in series can glow an LED and the capacitance retention is 94% after 1000 cycles (Figure 8e). Recently, Ficus religiosa's dead leaf derived porous carbon was also utilized as electrode material for fiber SCs [55b] and the maximum length energy density of 311 mWh kg^{-1} (37.3

x 10^{-8} Wh cm^{-1}) at a power density of 58 W kg^{-1} (70.3 µW cm^{-1}) was achieved. Moreover, a capacitance retention of 88% was obtained after 4000 cycles with demonstrated electrochemical performance at normal and bend conditions. Similarly, a specific capacitance of 45.2 mF cm^{-1} at 2 mV s^{-1}, an energy density of 6.5 µWh cm^{-1}, and a power density of 27.5 µW cm^{-1} were reported [55c] for an activated carbon coated CF based fiber SC.

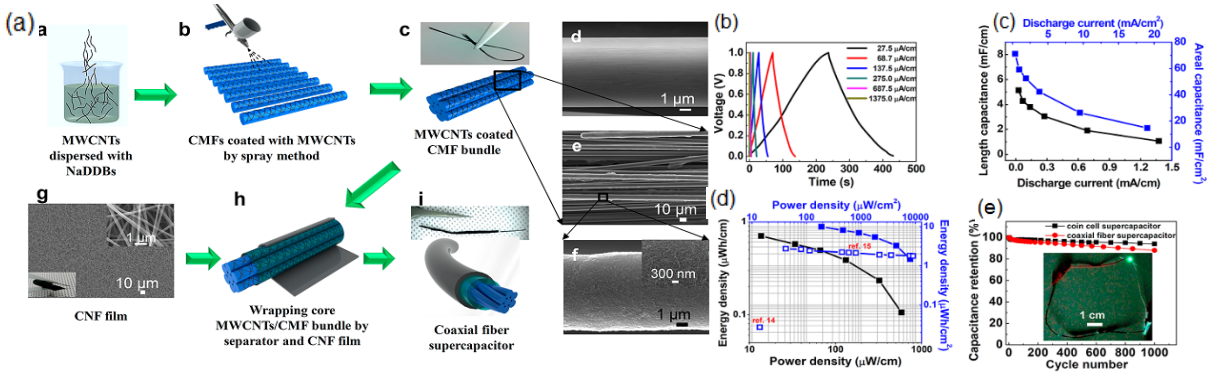

Figure 8 (a) Schematic of the coaxial fiber SC fabrication process, (b) charge-discharge curves at different current densities, (c) length specific capacitance as a function of current density, (d) Ragone plot with energy and power densities per length or per area of core-electrode and (e) cyclic performance of coaxial fiber SC and coin cell SC at a current density of 275 µA cm^{-1} (the inset is an LED lit by four coaxial fiber SCs connected in series, corresponding to 14.4 cm in length). Reproduced with permission [34].

In most reports, CF was used as the current collector. Interestingly, Zhou *et al*. [55d] used the CF as both fiber current collector and fiber electrode where the CF was modified via chemical oxidation. The oxidized CF showed a core shell structure and displayed excellent electrochemical performances. The CF fiber SC reaches a specific capacitance of 37.6 F g^{-1} and an energy density of 3.3 W h kg^{-1} (0.37 Wh cm^{-3}) at a power density of 122 W kg^{-1} (10.1 mW cm^{-3}). In this line, Yu *et al*. [55e] also modified the CF by chemical oxidation and reduction process and improved the surface area from 6 to 92 m^2 g^{-1}. Subsequently, the capacitance of the modified CF fiber electrode was increased from 0.6 to 14.2 F cm^{-3}. Finally, the fabricated modified CF based fiber SC showed a capacitance of 2.55 F cm^{-3} at 10 mV s^{-1} and an energy density of 0.35 mWh cm^{-3} at 3000 mW cm^{-3}. The reported work provides a low cost technique for large scale manufacturing of the device. However, the mechanical

strength of the CFs before and after modification was not studied [55d and 55e], which is a very important property for the durability of wearable devices.

4. Pseudocapacitive fiber SCs

In pseudocapacitive SCs (known as pseudocapacitors), charges are stored through fast faradic redox reactions (charge transfer reactions) on the surface of the electrode materials similar to the case in batteries, where the most commonly used electrode materials are metal oxides (RuO_2, MnO_2, Fe_2O_3, Fe_3O_4, and Co_3O_4, etc.) [56-58], metal hydroxides ($Ni(OH)_2$ and $Co(OH)_2$, etc.) [59,60] and conducting polymers (Polyaniline (PANI) [61] and Polypyrrole (PPy), etc.) [62]. The main advantage of those active materials is that they can provide higher specific capacitances [63] than carbon materials do due to the involving of multi-electron redox reactions within the operating potential window. For conventional SCs, pseudocapacitive electrode materials are extensively studied, while for fiber SCs, they are still in the initial stage of research.

Generally, it is difficult to fabricate the pseudocapacitive metal oxide and/or conducting polymers directly into fiber electrodes. Those active materials are normally coated on metal wire (such as Ni wire [64]), and/or carbon fiber current collector (such as CNT and/or graphene [14,24,65] fiber), which acts as a physical support to the metal oxides or conducting polymers. Table 2 summaries the recent results of pseudocapacitive fiber SCs where the metal oxides or conducting polymers were introduced to enhance the specific capacitance or energy density of the fiber SCs.

4.1. Metal wire@metal oxide based fiber SCs

Transition metal oxides have been extensively studied as electrodes for SC applications due to the high specific capacitance, large surface area, good redox property and controllable size

and shape. Generally, the pseduocapacitance depends on the potential difference or cell voltage which is given by $C = \Delta Q/\Delta V$, where ΔQ and ΔV indicate the stored charge and the potential window. The overall capacitance of a redox electrode is denoted as, $C = C_{dl} + C_{psed}$, where, C_{dl} is the ideal electric double layer (EDL) capacitance and C_{psed} is the pseduocapacitance because the electrode can store energy not only faradaically but also electrostatically [32,64].

To develop high performance fiber SCs, spinel based metal oxides (MCo_2O_4, where M=Ni, Zn, and Cu etc.,) have been used as electrode materials [66-68]. The electrochemical reaction of the spinel based metal oxides in fiber SCs can be described as,

$$2MCo_2O_4 + 2OH^- \leftrightarrow MCo_2O_4||OH^- + MCo_2O_4–OH \quad (2)$$

where, $MCo_2O_4||OH^-$ represents the electric double layer formed by the hydroxyl ion, and MCo_2O_4–OH represents the product formed by the cathode reaction involving the hydroxyl ion [66-68]. In 2014, Wang *et al*. [66] fabricated coaxial SCs (Figure 9) based on $NiCo_2O_4$ coated Ni wire because $NiCo_2O_4$ is an attractive spinel material with good electronic conductivity and superior electrochemical properties due to its redox cobalt and nickel ions. $NiCo_2O_4$ can be prepared in different morphologies on Ni wire with correspondingly different electrochemical performances. A high volume capacitance of 10.3 F cm^{-3} at a current of 0.08 mA, an energy density of 1.44 mWh cm^{-3} and a power density of 17 W cm^{-3} have been successfully achieved. Similarly, $ZnCo_2O_4$ nanorods can be grown on a Ni wire by a single-step hydrothermal process and were utilized as fiber electrodes for fiber SCs [67]. The fabricated SC achieved a specific capacitance of 10.9 F g^{-1} and an energy density of 76 mWh kg^{-1}. Later, Ni@$CuCo_2O_4$ wire was used as electrode to fabricate the coaxial-helix type fiber SC [68]. The specific capacitance and energy density were 11.09 F g^{-1} at 2mA and 1.42 mWh g^{-1} at 0.3409 W g^{-1}, respectively.

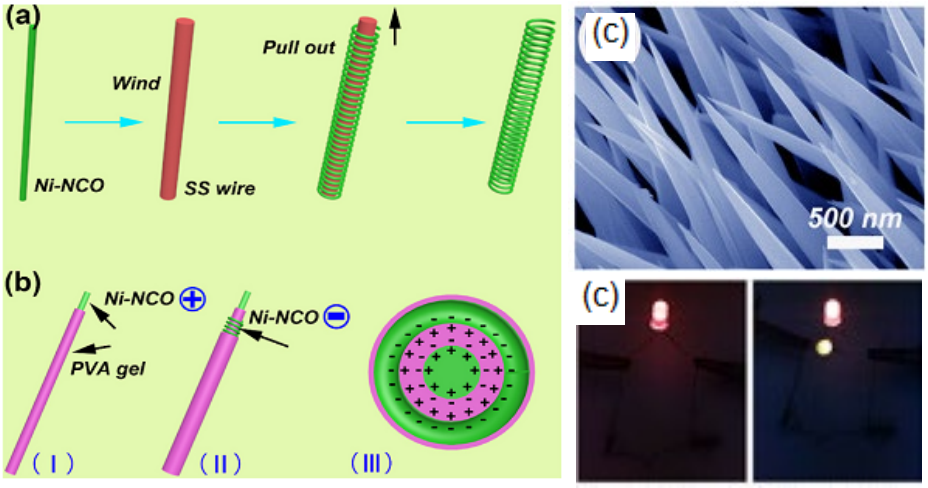

Figure 9 schematic diagrams showing (a) the fabrication of a winding electrode, (b) the fabrication process of a solid-state fiber SC, (c) SEM image of $NiCo_2O_4$ and (d) LED lit up by two SCs in series. Reproduced with permission [66].

4.2. Carbon fiber@metal oxide based fiber SCs

Incorporation or coating of metal oxides such as MnO_2, NiO and Co_3O_4 onto carbon fiber is an effective way to improve the performance of carbon based fiber SCs through additional pseudocapacitance. To introduce metal oxide onto a carbon fiber, electrodeposition was widely used [65,69,70] due to the simple process, time/energy saving and uniform coating formed on the fiber substrate. Ren *et al*. [65] have used an electrochemical method to deposit MnO_2 onto the MWCNT yarn (diameters from 2 to 30 μm and lengths up to 100 m) to enhance the performance of MWCNT based fiber SC, due to the high theoretical specific capacitance (1100–1300 F g^{-1}), low cost, environmental benignity and abundance of MnO_2. The MWCNT fiber was prepared by rotating spinning from a CNT forest and the fabricated fiber SC showed an area specific capacitance of 3.52 mF cm^{-2} (length specific capacitance of 0.019 mF cm^{-1}) at a current density of 5×10^{-4} mA. Likewise, Choi *et al*. [69] have coated MnO_2 on the porous MWCNT, where MnO_2 can be easily trapped into the 3D interconnected pores of the MWCNT matrix (Figure 10). The 3D porous structure provides excellent electrolytic surface area and a large amount of active sites of MnO_2 for better faradic reaction. Besides, it also provides short ion-diffusion length that facilitates full utilization of

MnO_2 even at high scan rate. Hence, a high specific capacitance of 25.4 F cm^{-3} at 10 mV s^{-1}, a high energy density of 3.52 mWh cm^{-3} and a high power density of 127 mW cm^{-3} have been achieved for the all-solid-state yarn SC. Independently, Su *et al*. [70] have coated Co_3O_4 and/or NiO onto the surface of CNT yarn by a simple electrodeposition process where the CNT yarn was prepared by CVD method. The capacitance of the Co_3O_4 yarn based SC was 52.6 mF cm^{-2} at 0.053 mA cm^{-2}, about 3.5 times that of the NiO yarn based SC (15.2 mF cm^{-2}).

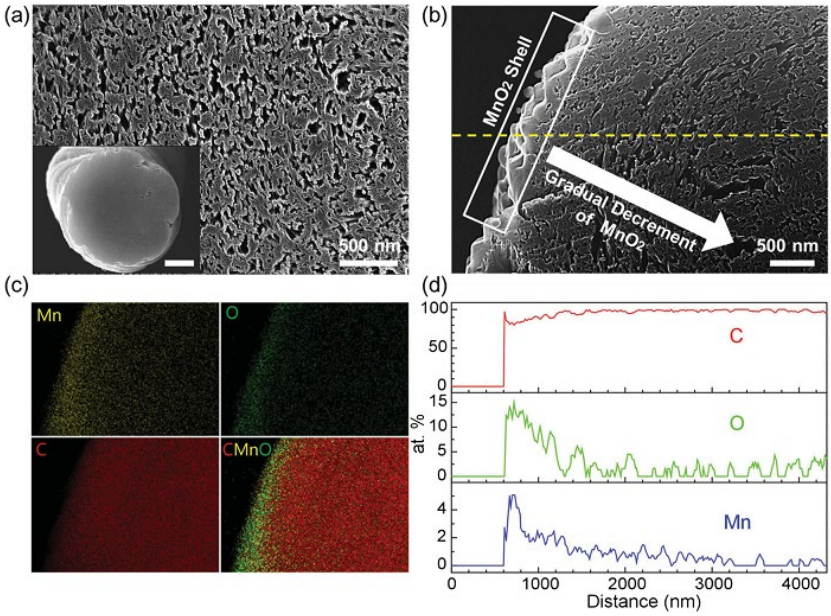

Figure 10 (a) Cross-sectional SEM image of CNT/MnO_2 fiber electrode (inset) and its magnified image, showing high internal porosity, (b) Magnified edge part of the CNT/MnO_2 fiber electrode (The core/shell (CNT/MnO_2) structure and direction of gradual concentration decrement of MnO_2 are shown), (c) Elemental mapping by energy dispersive spectroscopy (EDS) and (d) EDS line-scan data along the dashed line shown in (b). The presence of Mn and its gradual decrease along the canned line are confirmed. Reproduced with permission [69].

In addition, Chen *et al*. [24] prepared the MnO_2/graphene composite on graphene fiber to fabricate a fiber SC which showed a maximum specific capacitance of 9.6 mF cm^{-2}. The fiber SC demonstrated good electrochemical performances at both normal and bending states, revealing good flexible reliability of the device.

Table 2: Performance of recently reported pseudocapacitive fiber SCs

Device configuration (electrode material) and cell voltage	Electrolyte	Capacitance	Energy density and Power density	Cycle life	Ref.
Metal wire@metal oxide based fiber SCs					
Coaxial-helix ($NiCo_2O_4$) and 1 V	PVA-KOH	10.3 F cm^{-3}	1.44 mWh cm^{-3} and 17 W cm^{-3}	78 % for 5000 cycles	[66]
Coaxial-helix ($ZnCo_2O_4$) and 1 V	PVA-KOH	10.9 F g^{-1}	76 mWh kg^{-1} and 1.9 W g^{-1}	92 % for 3500 cycles	[67]
Coaxial-helix ($CuCo_2O_4$) and 1 V	PVA-KOH	11.09 F g^{-1}	1.42 Wh kg^{-1} and 0.3409 W g^{-1}	93.5 % for 4000 cycles	[68]
Carbon fiber@metal oxide based fiber SCs					
Parallel (MnO_2/MWCNT) and 2 V	$LiPF_6$/ethylene carbonate/diethyl carbonate/dimethyl carbonate	0.019 mF cm^{-1} or 3.57 mF cm^{-2}	1.73 mWh cm^{-3} and 0.79 W cm^{-3}	~97 % for 1000 cycles	[65]
Twisted (MnO_2/MWCNT) and 0.9 V	PVA-KOH	25.4 F cm^{-3}	3.52 mWh cm^{-3} and 127 mW cm^{-3}	---	[69]
Parallel (Co_3O_4/CNT)and 0.8 V	PVA-H_2SO_4	52. 6 mF cm^{-2}	1.10 μWh cm^{-2} and 0.01 mW cm^{-2}	91 % for 1000 cycles	[70]
Twisted (MnO_2/graphene) and 0.8 V	PVA-H_2SO_4	9.6 mF cm^{-2}	---	Stable performance	[24]
Carbon fiber@conducting polymer based SCs					
Twisted (CNT@PANI) and 0.8 V	PVA-H_2SO_4	38 mF cm^{-2}	---	91 % for 800 cycles	[14]
Twisted (MWCNT@PANI) and 0.8 V	PVA-H_3PO_4	274 F g^{-1} (or 263 mF cm^{-1})	---	99 % for 1000 cycles	[71]
Twisted (IR-CNT@PANI) and 1 V	PVA-H_3PO_4	78 F g^{-1} (43 mF cm^{-2})	---	89 % for 1000 cycles	[15]
Parrallel (IR-CNT@PEDOT/PSS) and 1 V	PVA-H_3PO_4	18.5 F g^{-1}	---	91 % for 600 cycles	[72]
Twisted (stretchable) (CNT@PPy) and 1 V	PVA-H_3PO_4	63.6 F g^{-1}	---	90 % for 1000 cycles	[73]

4.3. Carbon fiber@conducting polymer based fiber SCs

Conducting polymers are another kind of electrode materials to improve the electrochemical performance of carbon based fiber SCs due to their large capacitance, good electric conductivity, ease of synthesis, and low cost. Different types of conducting polymers, such as polyaniline (PANI), polypyrrole (PPy), and poly [3,4-ethylenedioxythiophene] (PEDOT),

have been widely studied in conventional planar SCs because they have very large specific capacitances, e.g., 1284 F/g for PANI, 480 F/g for PPy, and 210 F/g for PEDOT [74]. Commonly, there are two methods to synthesize conducting polymers i.e., chemical and electrochemical ones [74]. However, only few reports are available for the fabrication of conducting polymer based fiber SCs. Among them, PANI is the first to be used in fiber SCs since it possesses the largest theoretical capacitance due to its multiple redox states. Wang *et al*. first reported the conducting polymer-carbon composite based fiber SCs [14] using PANI nanowire arrays deposited CNT yarn (CNT@PANI) where in-situ polymerization was adopted to create PANI nanowires. The areal capacitance of CNT@PANI yarn-based SC (38 mF cm^{-2}) was much higher than that of the pure CNT yarn-based SC (2.3 mF cm^{-2}). Its capacitance retention was 91% even after 800 charge–discharge cycles. Cai *et al*. [71] reported an electrochemical deposition method to synthesize PANI based (CNT@PANI) fiber electrode using a simple three electrode system. The performance of the PANI based fiber electrode was tested by twisting two electrodes and a high specific capacitance of 274 F g^{-1} (or 263 mF cm^{-1}) was achieved. Moreover, at low loading amount of PANI, the capacitance measured under 2 A g^{-1} increased with increasing PANI amount, reaching a value of 4.5, 78, 114, 177 and 274 F g^{-1} at the PANI weight percentage of 0, 7.4, 19, 29, and 48%, respectively. However, further increase of the PANI to 70 wt.% decreased the specific capacitance to 245 F g^{-1}.

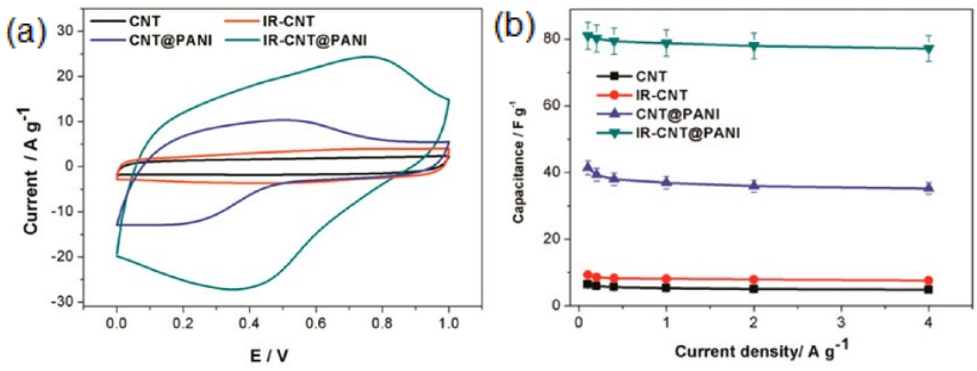

Figure 11 (a) Cyclic voltammograph (CV) curves at a scan rate of 0.5 V s^{-1} and (c) Specific capacitances at different current densities. Reproduced with permission [15].

The gamma-irradiated CNT (IR-CNT) yarn was used as a strong reinforcement and highly efficient current collector for fiber SC by Su *et al*. [15], where the CNT yarn was spun from a solid-state MWCNT forest. PANI was then coated on the IR-CNT yarn via a simple chemical method. Interestingly, the IR-CNT@PANI based fiber SC showed a large current area (Figure 11a) in CV curve, showing 10 times higher capacitance (78 F g^{-1}) than IR-CNT fiber SC (7.5 F g^{-1}) at 2.0 A g^{-1}, while the capacitance was 4.8 F g^{-1} for CNT yarn SC and 35.2 F g^{-1} for CNT@PANI yarn SC (Figure 11b). The same group also coated the gamma-irradiated CNT (IR-CNT) yarn with Poly(3,4-ethylenedioxythiophene)-poly(styrenesulfonate) (IR-CNT@PEDOT/PSS) [72] because PEDOT has good film forming property, high stability, and high conductivity and PEDOT/PSS improves the electroactivity due to the "doping effect" of PSS. However, the achieved capacitance (18.5 F g^{-1}) of IR-CNT@PEDOT/PSS based fiber SC was lower than that of the IR-CNT@PANI based fiber SC, even at low current density of 0.1 A g^{-1}.

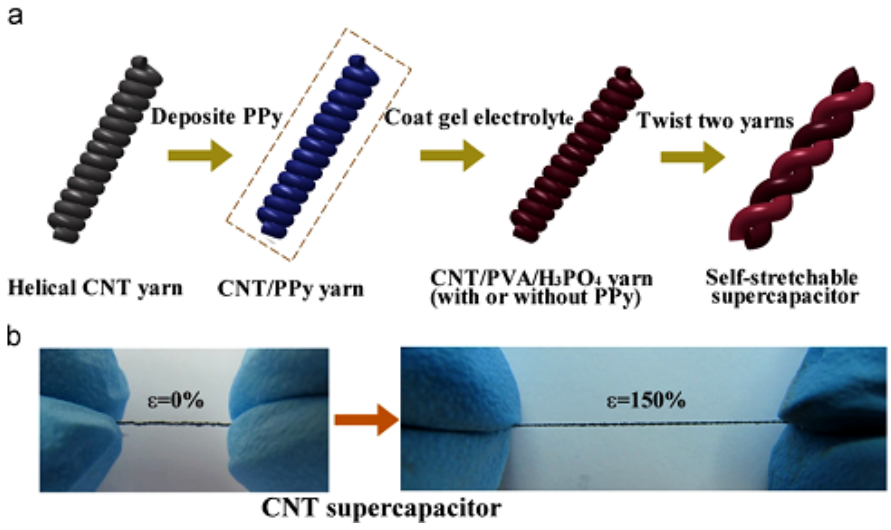

Figure 12 (a) Schematic fabrication process of a double-helix SC. (b) Snapshots of a double-helix CNT yarn SC manually stretched to 1.5 times of the original length. Reproduced with permission [73].

A novel self-stretchable fiber SC was fabricated based on PPy coated helical CNT yarn where the PPy was coated by electrochemical deposition. The helical loop structured CNT yarn provides the stretchable feature without additional stretchable substrate (Figure 12). The bare CNT based SC showed specific capacitances of only 18.1 and 19.2 F g^{-1} (at 100 mV s^{-1}) at normal and stretched states, respectively. Instead, the PPy coated helical CNT based SC showed a much higher specific capacitance of 63.6 F g^{-1} at 100 mV s^{-1} and the capacitance retention was around 90% after 1000 cycles [73].

5. Asymmetric fiber SCs

Symmetric fiber SCs have the shortcoming of low capacitance or lower energy density. To achieve better performance, asymmetric fiber SCs were developed [75–77]. Generally, most of the asymmetric SCs use asymmetric electrodes in the same cell, such as a pseudocapacitive electrode and an EDLC electrode. In this case, the pseudocapacitive electrode exhibits high energy density through its faradaic process and the EDLC electrode keeps high power density. Moreover, the energy density of an asymmetric SC is increased via the increasing working voltage which is almost the sum of the maximum potential windows of the negative and positive electrodes [78]. The working potential range of the positive and negative electrodes could be different. For example, the RGO/MWCNT electrode works [79] in a potential range from -0.1 to -0.9 V and it is used as the negative electrode, while the redox type electrode (carbon fiber paper-supported Polypyrrole, CFP/PPy) works from –0.1 to 0.7 V and it is used as the positive electrode (Figure 13a). Interestingly, the fabricated hybrid SC works with the sum of potential windows of the individual (positive and negative) electrode, i.e, 1.8 V. The CV curves and charge-discharge curves didn’t show any oxygen evolution and over charge regions even at a voltage up to 1.8 V (Figures 13 b and c), revealing a stable electrochemical performance in the full voltage window of the device. In

recent years, great efforts have been devoted to the enhancement of energy performance of fiber SCs by employing asymmetric designs as summarized in table 3.

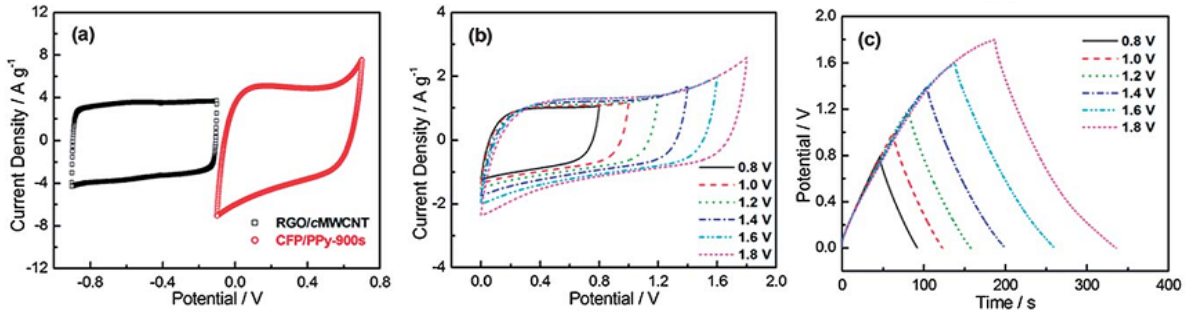

Figure 13 Electrochemical performance of CFP/PPy//RGO/MWCNT all solid-state asymmetric SC. (a) Cyclic voltammograms of RGO/MWCNT and CFP/PPy electrodes in a three-electrode systems at a scan rate of 20 mV s^{-1}, (b) cyclic voltammograms at different potential windows at a scan rate of 20 mV s^{-1} and (c) galvanostatic charge/discharge curves at different potential windows at a current density of 1 A g^{-1}. Reproduced with permission [79].

A high performance two-ply yarn (fiber) asymmetric SC has been designed for the first time in 2014 by Su *et al*. using as-spun CNT yarn as the negative electrode, CNT@MnO_2 composite yarn as the positive electrode and PAV-H_3PO_4 as the electrolyte [75]. This asymmetric SC works with the maximum cell voltage of 2 V and thus delivers the maximum specific capacitance of 17.5 F g^{-1} with an energy density of 42 Wh kg^{-1} at a power density of 483.7 W kg^{-1}. A similar asymmetric SC assembled with a core-sheathed MnO_2 coated graphene fiber and a graphene/CNT hybrid fiber in a PVA/LiCl gel electrolyte was developed by Zheng *et al*. [17] and an energy density of 11.9 μWh cm^{-2} (11.9 mWh cm^{-3}) was achieved. After 8000 cycles, the device still maintained about 92.7 % of its initial capacitance, demonstrating good cycling performances. Very recently, Xu *et al*. developed a coaxial-type fiber asymmetric SC (working voltage ~1.8V) [76a] by wrapping a MnO_2-modified nanoporous gold wire (NPG@MnO_2) with a conducting carbon paper and using PVA/LiCl electrolyte (Figure 14). The modified NPG wire provides an excellent support for MnO_2 with good flexibility, large tensile strength and superior electronic conductivity. A high

capacitance and a high energy density of 12 mF cm^{-2} and 5.4 μWh cm^{-2} were obtained, respectively. MnO_2–PPy and V_2O_5–PANI–carbon composite fiber electrodes were also fabricated to form an asymmetric fiber SC [76b], which can work in the potential ranges from 0 to 0.8 V and -0.8 to + 0.8 V, respectively. Hence, the asymmetric fiber SC delivered the maximum areal capacitance of 0.613 F cm^{-2} and energy density of 0.340 mWh cm^{-2} for the working voltage of 2 V. A drawback of this work was the use of liquid electrolyte (4 M LiCl) that could affect the unique properties of the fiber SCs as mentioned above. Similarly, Zhang *et al*. [56c] investigated the electrochemical performance of the hierarchically structured MnO_2/graphene/CF electrode and three-dimensional (3D) porous graphene hydrogel (GH) wrapped copper wire (CW) electrode for asymmetric fiber SC. The assembled device yields a high areal energy density of 18.1 mWh cm^{-2} and volumetric energy density of 0.9 mWh cm^{-3} for a voltage of 1.6 V. Nevertheless, the copper wire provides low flexibility to the device. Afterwards, a novel candidate [56d] was fabricated with functionalized carbon nanoparticle (FCNP)@CF as the negative electrode and MnO_2 nanosheet-CNP@CF as the positive electrode. A high discharge volumetric capacitance of 4.6 F cm^{-3} (at 0.25 A cm^{-3}) was obtained, which provided superior energy and power densities (2.1 mWh cm^{-3} and 8 W m^{-3}, respectively).

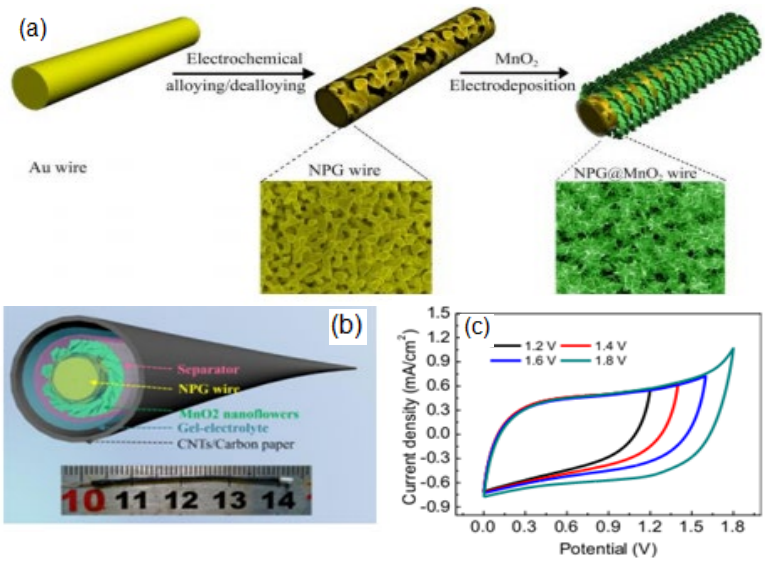

Figure 14 (a) Schematic illustration of the synthesis and morphology of the NPG@MnO_2 electrode, (b) schematic diagram of a coaxial fiber asymmetric SC (inset: a photograph of the device) and (c) CV curves of the as-assembled device in different voltage windows. Reproduced with permission [76].

A solid-state asymmetric fiber SC was fabricated by Dong *et al*. [25] by twisting a $Ni(OH)_2$-nanowire fiber electrode and an ordered mesoporous carbon (OMC) coated fiber electrode with a PVA-KOH gel polymer electrolyte. During an electrochemical test, the following reactions (or processes) could occur on the positive and negative electrodes in the fiber SC.

$$2\beta\text{-}Ni(OH)_2 + OH \leftrightarrow 2NiOOH + H_2O + e^- \text{ (positive electrode)} \quad (3)$$

$$OMC + xK^+ \leftrightarrow OMC||xK^+ \quad \text{(negative electrode)} \quad (4)$$

where, || indicates the EDL, the positive electrode provides the capacitance via redox reaction and the negative electrode provides the capacitance via EDL process. The fabricated asymmetric architecture allows an operating voltage up to 1.5 V. A specific capacitance of 6.67 mF cm^{-1} (35.67 mF cm^{-2}) and a specific energy density of 0.01 mWh cm^{-2} (2.16 mWh cm^{-3}) were achieved with 70% of capacitance retention after over 10000 cycles. We have also fabricated a cable-type asymmetric SC (working voltage ~ 1.4 V), using plate-like $Ni(OH)_2$ as the positive electrode, activated carbon as the negative electrode and PVA–KOH gel polymer as the electrolyte [6]. The plate-like $Ni(OH)_2$ was prepared by a reflux method and the activated carbon was derived from Tamarindus indica fruit shell. This asymmetric cable SC has a capacitances of 40.7 mF cm^{-1} (37.5 F g^{-1}) and an energy density of 10.7 μWh cm^{-1} (9.8 Wh kg^{-1}) at a power density of 169 mW cm^{-1} (154 W kg^{-1}).

A novel asymmetric fiber SC fabricated [77] with Co_3O_4 nanowires (positive electrode) and graphene (negative electrode) yielded a volumetric capacitance of 2.1 F cm^{-3}, an energy density of 0.62 mW h cm^{-3} and a power density of 1.47 W cm^3. After 1000 cycles, the

maximum capacitance was 1.59 F cm^{-3} with 16 % loss of the initial value. Very recently, functionalized

Table 3: Performance of recently reported asymmetric fiber supercapacitors

Electrode		Device configuration and cell voltage	Electrolyte	Capacitance	Energy density and Power density	Cycle life	Ref.
Positive	Negative						
$Ni(OH)_2$	Activated carbon	Parallel and 1.4 V	PVA-KOH	40.7 mF cm^{-1} (37.5 F g^{-1})	10.7 μWh cm^{-1} (9.8 Wh kg^{-1}) and 169 μW cm^{-1} (154 W kg^{-1}).	76 % for 2000 cycles	[6]
MnO_2@graphene fiber	Graphene/CNT hybrid fiber	Twisted and 1.6 V	PVA-LiCl	19.1 mF cm^{-2}	11.9 μWh cm^{-2} (11.9 mWh cm^{-3})	92.7 % for 8000 cycles	[17]
Ni wire@$Ni(OH)_2$	Ordered mesoporous carbon (OMC)	Coaxial-helix and 1.5 V	PVA-KOH	6.67 mF cm^{-1} (35.67 mF cm^{-2})	0.01 mWh cm^{-2} (2.16 mWh cm^{-3}) and 7.3 mW cm^{-2} (1600 mW cm^{-3})	70 % for 10000 cycles	[25]
CNT@MnO_2 composite yarn	CNT yarn	Twisted and 2.0 V	PAV-H_3PO_4	17.5 F g^{-1}	42 Wh kg^{-1} and 483.7 W kg^{-1}	99 % for 500 cycles	[75]
Nanoporous gold wire@MnO_2	Carbon paper	Coaxial and 1.8 V	PVA-LiCl	12 mF cm^{-2}	5.4 μWh cm^{-2} and 284 μW cm^{-2}	90 % for 2000 cycles	[76a]
MnO_2–PPy@carbon fiber	V_2O_5–PANI@carbon fiber	Parallel and 2 V	LiCl solution	0.613 F cm^{-2}	0.340 mWh cm^{-2} and 1.5 mW cm^{-2}	---	[76b]
MnO_2/graphene@carbon fiber	Graphene hydrogel @copper wire	Coaxial and 1.6 V	Potassium polyacrylate (PAAK)/KCl	2.54 F cm^{-3} (50.8 mF cm^{-2})	18.1 mWh cm^{-2} (0.9 mWh cm^{-3})	84% for 10 000 cycles	[76c]
MnO_2 nanosheet-carbon nanoparticle (CNP)@CF	Functionalized CNP@CF	Parallel and 1.8 V	LiCl/PVA	4.6 F cm^{-3}	2.1 mWh cm^{-3}, 8 W m^{-3}	81.2% for 10000	[76d]
Ni wire@Co_3O_4	Graphene	Coaxial-helix and 1.5 V	PVA-KOH	2.1 F cm^{-3}	0.62 mW h cm^{-3} and 1.47 W	84 % for 1000	[77]

					cm^{-3}	cycles	
Carbon fiber@PANI	Functionalized carbon fiber	Twisted and 1.6 V	PAV-H_3PO_4	4.8 F cm^{-3}	2 mWh cm^{-3} and 11 W cm^{-3}	81 % for 10000 cycles	[80]

carbon fiber thread and carbon fiber@PANI thread were used as negative and positive electrodes, respectively, to make the asymmetric fiber SC with PVA-H_3PO_4 gel electrolyte. In this work, the coating of PANI on carbon fiber thread and the functionalization of carbon fiber thread were realized through electrochemical technique in a simple three electrode system. The fabricated SC exhibited excellent electrochemical performance, such as, a high capacitance of 4.8 F cm^{-3} and a high energy density of 2 mWh cm^{-3}, with the maximum working voltage of 1.6 V [80].

Summary

In this review, we have focused on the recent progress and advances of fiber SCs in terms of their design, configuration and electrode materials. Fiber SC is a fast growing candidate in energy storage devices and many new innovations have emerged for advanced flexible wearable/stretchable applications. Fiber SCs are highly flexible and can be fixed into very small space or woven into textiles when compared with the conventional planar type flexible SCs. The recently developed carbon fiber, CNT fiber and graphene fiber provide more flexibility than the metal coated plastic wire or metal wire used as current collectors in early stage fiber SCs. Gel electrolyte emerged to be an important component in various SC architectures, such as parallel-like type, coaxial type, two-ply type, coaxial-helix type and all-in one type. Significant advances have been made to improve the performance of carbon based fiber SCs through the introduction of pseudocapacitive materials, such as metal oxides and conducting polymers. By constructing asymmetric SCs, further improvement in the energy density can be achieved with higher voltage. Overall, remarkable progresses have

been made on fiber SCs in an effort to achieve high energy density.

Challenges and future perspective

For practical applications of fiber SCs, challenges remain which call for further fundamental research and development. For examples, H_3PO_4 and KOH based gel electrolytes are widely used in fiber SCs. However, little attention was paid to the device encapsulation which is highly risky in wearable applications since H_3PO_4 and KOH are corrosive. When encapsulation is considered, the device may lose many of its attractive features of light weight, small size, mechanical stability, flexibility, as well as its energy density and power density. The rapid development of fiber SCs also calls for standard characterization technique of the device and standard parameters to be used to evaluate and compare the performances of various types of devices. Presently, there is no standard procedure to characterize the performance of fiber SCs whose capacity, energy density and power density are reported in different units (volumetric (cm^{-3}), length (cm^{-1}) or areal (cm^{-2})) (see Tables 1-3). In addition, the balance of charges on positive and negative electrodes is very important for the fabrication of asymmetric fiber SCs. However, there is no standard procedure to balance the charges and currently the charges are normally balanced by either gravimetric or volumetric capacitances in the available reports. Moreover, self-discharge or leakage current is one of the major problems in conventional SCs. For practical applications of fiber SCs, systematic studies of self-discharge or leakage current should be conducted on fiber SCs.

The energy densities of fiber SCs are still very low compared with other available micro-sized energy storage devices like batteries. One of the limiting factors is the aqueous based gel electrolyte used which limits the working voltage of the device. Urgent attention should be paid to the development of gel electrolytes that improve the cell voltage. In this context, the use of ionic liquid or organic electrolyte based polymer electrolyte is a very

effective approach to high energy and power densities of fiber SCs. However, issues such as cost and toxicity should be considered. The combination of SC and battery is another way to achieve higher energy and power densities. In such a hybrid SC (HSC), one electrode can store the charges via a process similar in a capacitor which provides a high power density to the device and the other electrode can store the charges via a faradaic process (similar to a battery) which provides a high energy density. Of course, the identification of high performance electrode is always an important research direction to improve the energy density.

So far, only very few reports have been demonstrated for stretchable fiber SCs which are mainly of a symmetric type. Much more efforts should be paid to the design of asymmetric stretchable fiber SCs which have a high voltage. The design and optimization of different SC architectures should also be paid considerable attention to attain high performance fiber SCs for practical applications. The coupling and integration of fiber SCs to available fiber electronic devices, such as transistors, sensors, fuel cells, solar cells, thermoelectric power generators and piezoelectric generators (nanogenerators) is in its infancy and will boost in the future, in view of the huge commercial market in wearable electronics. Many of the breakthroughs to be made in the above mentioned directions still rely on the development of materials science and engineering that will eventually lead to the practical applications of fiber SCs.

Acknowledgements:

This work is supported by the Research Grants Council of the Hong Kong Special Administrative Region, China (Project Nos. M-PolyU503/13 and PolyU5159/13E).

References:

[1] J. Jang, *Mater. Today*, 2006, **9**, 46-52.

[2] M. Segev-Bar and H. Haick, *ACS Nano*, 2013, **7**, 8366-8378.

[3] D. Shahrjerdi and S.W. Bedell, *Nano Lett.*, 2013, **13**, 315-320.

[4] S.J. Kim, J.H. We and B.J. Cho, *Energy Environ. Sci.*, 2014, **7**, 1959-1965.

[5] S. Das, R. Gulotty, A. V Sumant and A. Roelofs, *Nano Lett.*, 2014, **14**, 2861-2866.

[6] S.T. Senthilkumar and R. Kalai Selvan, *Phys. Chem. Chem. Phys.*, 2014, **16**, 15692-15698.

[7] X. Yu, Y. Fu, X. Cai, H. Kafafy, H. Wu, M. Peng, S. Hou, Z. Lv, S. Ye and D. Zou, *Nano Energy*, 2013, **2**, 1242-1248.

[8] W. Zeng, L. Shu, Q. Li, S. Chen, F. Wang and X.-M. Tao, *Adv. Mater.*, 2014, **26**, 5310-5336.

[9] L. Li, Z. Wu, S. Yuan and X.-B. Zhang, *Energy Environ. Sci.*, 2014, **7**, 2101-2122.

[10] P. Yang and W. Mai, *Nano Energy*, 2014, **8**, 274-290.

[11] Z. Liu, J. Xu, D. Chen and G. Shen, *Chem. Soc. Rev.*, 2015, **44**, 161-192.

[12] G. Zhou, F. Li and H.-M. Cheng, *Energy Environ. Sci.*, 2014, **7**, 1307-1338.

[13] X. Cai, M. Peng, X. Yu, Y. Fu and D. Zou, *J. Mater. Chem. C*, 2014, **2**, 1184-1200.

[14] K. Wang, Q. Meng, Y. Zhang, Z. Wei and M. Miao, *Adv. Mater.*, 2013, **25**, 1494-1498.

[15] F. Su, M. Miao, H. Niu and Z. Wei, *ACS Appl. Mater. Interfaces*, 2014, **6**, 2553-2560.

[16] Y. Fu, X. Cai, H. Wu, Z. Lv, S. Hou, M. Peng, X. Yu and D. Zou, *Adv. Mater.*, 2012, **24**, 5713-5718.

[17] B. Zheng, T. Huang, L. Kou, X. Zhao, K. Gopalsamy and C. Gao, *J. Mater. Chem. A*, 2014, **2**, 9736-9743.

[18] Y. Cao, M. Zhu, P. Li, R. Zhang, X. Li, Q. Gong, K. Wang, M. Zhong, D. Wu, F. Lin and H. Zhu, *Phys. Chem. Chem. Phys.*, 2013, **15**, 19550-19556.

[19] J. Bae, M.K. Song, Y.J. Park, J.M. Kim, M. Liu and Z.L. Wang, *Angew. Chem. Int. Ed.*, 2011, **50**, 1683-1687.

[20] X. Lu, M. Yu, G. Wang, Y. Tong and Y. Li, *Energy Environ. Sci.*, 2014, **7**, 2160-2181.

[21] S.T. Senthilkumar, R.K. Selvan, N. Ponpandian and J.S. Melo, *RSC Adv.*, 2012, **2**, 8937-8940.

[22] N.A. Choudhury, S. Sampath and A.K. Shukla, *Energy Environ. Sci.*, 2009, **2**, 55-67.

[23] D. Harrison, F. Qiu, J. Fyson, Y. Xu, P. Evans and D. Southee, *Phys. Chem. Chem. Phys.*, 2013, **15**, 12215-12219.

[24] Q. Chen, Y. Meng, C. Hu, Y. Zhao, H. Shao, N. Chen and L. Qu, *J. Power Sources*, 2014, **247**, 32-39.

[25] X. Dong, Z. Guo, Y. Song, M. Hou, J. Wang, Y. Wang and Y. Xia, *Adv. Funct. Mater.*, 2014, **24**, 3405-3412.

[26] Y. Hu, H. Cheng, F. Zhao, N. Chen, L. Jiang, Z. Feng and L. Qu, *Nanoscale*, 2014, **6**, 6448-6451.

[27] Z. Yang, J. Deng, X. Chen, J. Ren and H. Peng, *Angew. Chem. Int. Ed.*, 2013, **52**, 13453-13457.

[28] (a) T. Chen and L. Dai, *J. Mater. Chem. A*, 2014, **2**, 10756-10775; (b) Q. Wang, J. Yan, Y. Wang, T. Wei, M. Zhang, X. Jing, Z. Fan, *Carbon*, 2014, **67**, 119-127.

[29] L.L. Zhang and X.S. Zhao, *Chem. Soc. Rev.*, 2009, **38**, 2520-2531.

[30] X. Zhang, H. Zhang, C. Li, K. Wang, X. Sun and Y. Ma, *RSC Adv.*, 2014, **4**, 45862-45884.

[31] S.T. Senthilkumar, R.K. Selvan, J.S. Melo and C. Sanjeeviraja, *ACS Appl. Mater. Interfaces*, 2013, **5**, 10541-10550.

[32] (a) G. Wang, L. Zhang and J. Zhang, *Chem. Soc. Rev.*, 2012, **41**, 797-828; (b) W. Xing, C. C. Huang, S. P. Zhuo, X. Yuan, G. Q. Wang, D. Hulicova-Jurcakova, Z.F. Yan, G. Q. Lu, *Carbon*, 2009, **47**, 1715-1722.

[33] X. Chen, L. Qiu, J. Ren, G. Guan, H. Lin, Z. Zhang, P. Chen, Y. Wang and H. Peng, *Adv. Mater.*, 2013, **25**, 6436-6441.

[34] V.T. Le, H. Kim, A. Ghosh, J. Kim, J. Chang, Q.A. Vu, D.T. Pham, J.H. Lee, S.W. Kim and Y.H. Lee, *ACS Nano*, 2013, **7**, 5940-5947.

[35] W. Zhou, K. Zhou, X. Liu, R. Hu, H. Liu and S. Chen, *J. Mater. Chem. A*, 2014, **2**, 7250-7255.

[36] J. Ren, W. Bai, G. Guan, Y. Zhang and H. Peng, *Adv. Mater.*, 2013, **25**, 5965-5970.

[37] D. Yu, K. Goh, Q. Zhang, L. Wei, H. Wang, W. Jiang and Y. Chen, *Adv. Mater.*, 2014, **26**, 6790-6797.

[38] Z. Zhang, X. Chen, P. Chen, G. Guan, L. Qiu, H. Lin, Z. Yang, W. Bai, Y. Luo and H. Peng, *Adv. Mater.*, 2014, **26**, 466-470.

[39] W. Lu, M. Zu, J.H. Byun, B.S. Kim and T.W. Chou, *Adv. Mater.*, 2012, **24**, 1805-1833.

[40] H. Sun, X. You, J. Deng, X. Chen, Z. Yang, J. Ren and H. Peng, *Adv. Mater.*, 2014, **26**, 2868-2873.

[41] P. Xu, T. Gu, Z. Cao, B. Wei, J. Yu, F. Li, J.H. Byun, W. Lu, Q. Li and T.W. Chou, *Adv. Energy Mater.*, 2014, **4**, 1300759-1300764.

[42] (a) C. Liu, Z. Yu, D. Neff, A. Zhamu and B.Z. Jang, *Nano Lett.*, 2010, **10**, 4863-4868; (b) H. Lei, T. Yan, H. Wang, L. Shi, J. Zhang and D. Zhang, *J. Mater. Chem. A,* 2015, **3**, 5934-5941; (c) H. Wang, L. Shi, T. Yan, J. Zhang, Q. Zhong and D. Zhang, *J. Mater. Chem. A*, 2014, **2**, 4739-4750; (d) H. Wang, D. Zhang, T. Yan X. Wen, J. Zhang, L. Shi and Q. Zhong, *J. Mater. Chem. A*, 2013, **1**, 11778-11789.

[43] J. Xia, F. Chen, J. Li and N. Tao, *Nat. Nanotechnol.*, 2009, **4**, 505-509.

[44] R. Trusovas, K. Ratautas, G. Račiukaitis, J. Barkauskas, I. Stankevičiene, G. Niaura and R. Mažeikiene, *Carbon*, 2013, **52**, 574-582.

[45] K.S. Novoselov, V.I. Fal'ko, L. Colombo, P.R. Gellert, M.G. Schwab and K. Kim, *Nature*, 2012, **490**, 192-200.

[46] X. Su, G. Wang, W. Li, J. Bai and H. Wang, *Adv. Powder Technol.*, 2013, **24**, 317-323.

[47] X. Huang, X. Qi, F. Boey and H. Zhang, *Chem. Soc. Rev.*, 2012, **41**, 666-686.

[48] (a) Y. Li, K. Sheng, W. Yuan and G. Shi, *Chem. Commun.*, 2013, **49**, 291-293; (b) L. Liu, Y. Yu, C. Yan, K. Li and Z. Zheng, *Nat. Comm.,* 2015, **6**, 7260.

[49] H. Cheng, C. Hu, Y. Zhao and L. Qu, *NPG Asia Mater.*, 2014, **6**, e113.

[50] Y. Meng, Y. Zhao, C. Hu, H. Cheng, Y. Hu, Z. Zhang, G. Shi and L. Qu, *Adv. Mater.*, 2013, **25**, 2326-2331.

[51] Q. Ji, X. Zhao, H. Liu, L. Guo and J. Qu, *ACS Appl. Mater. Interfaces*, 2014, **6**, 9496-9502.

[52] X. Zhao, B. Zheng, T. Huang and C. Gao, *Nanoscale*, 2015, **7**, 9399-9404.

[53] L. Kou, T. Huang, B. Zheng, Y. Han, X. Zhao, K. Gopalsamy, H. Sun and C. Gao, *Nat. Commun.*, 2014, **5**, 3754-3763.

[54] J. Foroughi, G.M. Spinks, D. Antiohos, A. Mirabedini, S. Gambhir, G.G. Wallace, S.R. Ghorbani, G. Peleckis, M.E. Kozlov, M.D. Lima and R.H. Baughman, *Adv. Funct. Mater.*, 2014, **24**, 5859-5865.

[55] (a) H. Cheng, Z. Dong, C. Hu, Y. Zhao, Y. Hu, L. Qu, N. Chen and L. Dai, *Nanoscale*, 2013, **5**, 3428-3434; (b) S. T. Senthilkumar and R. Kalai Selvan, *ChemElectroChem*, 2015, **2**, 1111-1116; (c) S. Zhai, W. Jiang, L. Wei, H. E. Karahan, Y. Yuan, A. K. Ng, Y. Chen, *Mater. Horiz.*, 2015, DOI: 10.1039/C5MH00108K; (d) W. Zhou,. K. Zhou, X. Liu, R. Hu, H. Liu and S. Chen, *J. Mater. Chem. A*, 2014, **2**, 7250-7255; (e) D. Yu, S. Zhai, W. Jiang, K. Goh, L. Wei, X Chen, R. Jiang, and Y. Chen, *Adv. Mater.* 2015, DOI: 10.1002/adma.201501948.

[56] K. Xie, J. Li, Y. Lai, W. Lu, Z. Zhang, Y. Liu, L. Zhou and H. Huang, *Electrochem. Commun.*, 2011, **13**, 657-660.

[57] K. Xie, Z. Lu, H. Huang, W. Lu, Y. Lai, J. Li, L. Zhou and Y. Liu, *J. Mater. Chem.*, 2012, **22**, 5560-5567.

[58] X. Li, Y. Chen, H. Yao, X. Zhou, J. Yang, H. Huang, Y.-W. Mai and L. Zhou, *RSC Adv.*, 2014, **4**, 39906-39911.

[59] M. Jin, G. Zhang, F. Yu, W. Li, W. Lu and H. Huang, *Phys. Chem. Chem. Phys.*, 2013, **15**, 1601-1605.

[60] G. Zhang, W. Li, K. Xie, F. Yu and H. Huang, *Adv. Funct. Mater.*, 2013, **23**, 3675-3681.

[61] K. Xie, J. Li, Y. Lai, Z. Zhang, Y. Liu, G. Zhang and H. Huang, *Nanoscale*, 2011, **3**, 2202-2207.

[62] S.T. Senthilkumar, R.K. Selvan and J.S. Melo, *J. Mater. Chem. A*, 2013, **1**, 12386-12394.

[63] S. Bose, T. Kuila, A.K. Mishra, R. Rajasekar, N.H. Kim and J.H. Lee, *J. Mater. Chem.*, 2012, **22**, 767-784.

[64] X. Zhao, B.M. Sánchez, P.J. Dobson and P.S. Grant, *Nanoscale*, 2011, **3**, 839-855.

[65] J. Ren, L. Li, C. Chen, X. Chen, Z. Cai, L. Qiu, Y. Wang, X. Zhu and H. Peng, *Adv. Mater.*, 2013, **25**, 1155-1159.

[66] Q. Wang, X. Wang, J. Xu, X. Ouyang, X. Hou, D. Chen, R. Wang and G. Shen, *Nano Energy*, 2014, **8**, 44-51.

[67] H. Wu, Z. Lou, H. Yang and G. Shen, *Nanoscale*, 2015, **7**, 1921-1926.

[68] S. Gu, Z. Lou, X. Ma and G. Shen, *ChemElectroChem*, 2015, DOI: 10.1002/celc.201500020 .

[69] C. Choi, J.A. Lee, a. Y. Choi, Y.T. Kim, X. Leprõ, M.D. Lima, R.H. Baughman and S.J. Kim, *Adv. Mater.*, 2014, **26**, 2059-2065.

[70] F. Su, X. Lv and M. Miao, *Small*, 2015, **11**, 854-861.

[71] Z. Cai, L. Li, J. Ren, L. Qiu, H. Lin and H. Peng, *J. Mater. Chem. A*, 2013, **1**, 258-261.

[72] F. Su and M. Miao, *Electrochim. Acta*, 2014, **127**, 433-438.

[73] Y. Shang, C. Wang, X. He, J. Li, Q. Peng, E. Shi, R. Wang, S. Du, A. Cao and Y. Li, *Nano Energy*, 2015, **12**, 401-409.

[74] K. Wang, H. Wu, Y. Meng and Z. Wei, *Small*, 2014, **10**, 14-31.

[75] F. Su and M. Miao, *Nanotechnology*, 2014, **25**, 135401.

[76] (a) H. Xu, X. Hu, Y. Sun, H. Yang, X. Liu and Y. Huang, *Nano Res.*, 2015, **8**, 1148-1158; (b) W. Liu, N. Liu, Y. Shi, Y. Chen, C. Yang, J. Tao, S. Wang, Y. Wang, Jun Su, L. Li and Y. Gao, *J. Mater. Chem. A*, 2015, **3**, 13461-13467; (c) Z. Zhang, F. Xiao and S. Wang, *J. Mater. Chem. A*, 2015, **3**, 11215-11223; (d) H. Jin, L. Zhou, C. Leung Mak, H. Huang, W. Man Tang and H. L. Wa Chan, *J. Mater. Chem. A*, 2015, **3**, 15633-15641.

[77] X. Wang, B. Liu, R. Liu, Q. Wang, X. Hou, D. Chen, R. Wang and G. Shen, *Angew. Chem. Int. Ed.*, 2014, **53**, 1849-1853.

[78] J. Zhang and X.S. Zhao, *ChemSusChem*, 2012, **5**, 818-841.

[79] C. Yang, J. Shen, C. Wang, H. Fei, H. Bao and G. Wang, *J. Mater. Chem. A*, 2014, **2**, 1458-1464.

[80] H. Jin, L. Zhou, C.L. Mak, H. Huang, W.M. Tang and H.L.W. Chan, *Nano Energy*, 2015, **11**, 662-670.